Molecular Plant Pathology

WILEY

Molecular Plant Pathology

ORIGINAL ARTICLE OPEN ACCESS

Hop Stunt Viroid Expression and Host Responses in *Arabidopsis thaliana*

Xiaxia Tian[1,2] | Binhui Zhan[1] | Lingzhu He[1] | Changyong Zhou[2] | Yunlong Ma[3] | Shifang Li[1,3] | Zhixiang Zhang[1]

[1]State Key Laboratory for Biology of Plant Diseases and Insect Pests, Institute of Plant Protection (IPP), Chinese Academy of Agricultural Sciences (CAAS), Beijing, China | [2]Citrus Research Institute, Southwest University, Chongqing, China | [3]Center for Biosafety, Chinese Academy of Inspection and Quarantine, Sanya, Hainan Province, China

Correspondence: Zhixiang Zhang (zhangzhixiang02@caas.cn) | Shifang Li (sfli@ippcaas.cn)

Received: 14 January 2025 | **Revised:** 22 February 2025 | **Accepted:** 12 March 2025

Funding: This work was supported by the National Nature Science Foundation of China, 32072395.

Keywords: *Arabidopsis thaliana* | replication | RNA silencing | viroid–host interactions | viroids

ABSTRACT

Arabidopsis thaliana serves as an appealing model for viroid research, though prior infection trials have largely failed. Previous studies have shown that mature circular RNAs of certain viroids can be synthesised in *A. thaliana* via transgenic methods. Here, we confirm this by introducing a transgene encoding the dimeric cDNA of hop stunt viroid (HSVd) genome and explore the potential of HSVd-expressing transgenic *A. thaliana* in viroid research. Mature HSVd circular genome RNA was detected in transgenic plants but accumulated to relatively low levels. Small RNA (sRNA) sequencing revealed minimal production of HSVd-derived sRNAs, suggesting inefficient replication. This finding highlights the importance of double-stranded replication intermediates as the primary source of viroid sRNAs. Moreover, the low replication efficiency increases the likelihood of identifying viroid-binding host factors involved in early molecular interactions using transgenic *A. thaliana*. Transcriptome analysis indicated that HSVd expression significantly altered the expression of thousands of *A. thaliana* genes, with enrichment in metabolic pathways, biosynthesis, plant hormone signalling, plant–pathogen interactions and MAPK signalling pathways. Interestingly, these pathways align with those observed in cucumber systemically infected with HSVd, suggesting that transgenic *A. thaliana* mimics systemic viroid infections and offers a promising model for studying viroid–host interactions. Thus, despite the challenges of establishing systemic infection, HSVd-expressing transgenic *A. thaliana* represents a valuable tool for advancing viroid research.

1 | Introduction

Viroids are small, single-stranded, circular RNAs that infect higher plants. These naked RNA molecules, with genomes under 450 nucleotides, lack protein-coding capacity, relying entirely on host machinery for their replication and life cycle (Navarro et al. 2021). Viroids can cause severe diseases in susceptible plants, yet the molecular mechanisms underlying viroid–host interactions remain poorly understood.

Due to its short life cycle, well-annotated genome, and extensive mutant library, *Arabidopsis thaliana* has been widely used to study virus–host interactions (Somerville and Koornneef 2002). However, its application in viroid research is limited, as most inoculation attempts have failed (Daros and Flores 2004). For instance, several pospiviroids were undetectable in systemic leaves after agroinfiltration, probably due to inefficient replication or impaired movement (Daros and Flores 2004). Interestingly, a recent study demonstrated that *A. thaliana* could be systemically infected by hop latent viroid (HLVd) via mechanical inoculation, resulting in stunting and chlorosis symptoms (Atallah et al. 2024), suggesting that systemic viroid infection in *A. thaliana* is achievable under specific conditions.

This is an open access article under the terms of the Creative Commons Attribution-NonCommercial License, which permits use, distribution and reproduction in any medium, provided the original work is properly cited and is not used for commercial purposes.

© 2025 The Author(s). *Molecular Plant Pathology* published by British Society for Plant Pathology and John Wiley & Sons Ltd.

Arabidopsis thaliana supports critical steps in viroid replication, including cleavage and ligation. Transgenes encoding dimeric viroid genomes have successfully produced mature circular viroid RNAs and replication intermediates in *A. thaliana* (Daros and Flores 2004). This transgenic approach has been instrumental in uncovering the molecular mechanisms of viroid replication and identifying host ligases involved in the process (Gas et al. 2007; Nohales et al. 2012). However, the broader host responses to viroid expression in *A. thaliana* and the utility of transgenic lines for studying viroid–plant interactions remain underexplored.

In this study, we generated transgenic *A. thaliana* expressing hop stunt viroid (HSVd) circular genome RNA. Transcriptome analysis revealed that HSVd expression significantly affects gene expression, particularly in pathways related to plant metabolism, hormone signalling, pathogen interactions and MAPK signalling. These changes closely resemble responses in HSVd-infected cucumber, indicating that transgenic *A. thaliana* could serve as a viable model for studying viroid–host interactions. Additionally, small RNA (sRNA) profiling showed minimal HSVd-derived sRNAs, suggesting inefficient viroid replication. Finally, crosses between HSVd-expressing plants and DICER-LIKE proteins (DCL) (*dcl2*, *dcl3*, *dcl4*, *dcl2/3*, *dcl2/4*, *dcl3/4* and *dcl2/3/4*) mutants demonstrated the complex roles of DCL proteins in viroid accumulation and defence.

2 | Results

2.1 | Inoculation of *A. thaliana* With Viroids

To evaluate the infectivity of HLVd in *A. thaliana* (Atallah et al. 2024), *A. thaliana* (ecotype Col-0) plants were inoculated with *Agrobacterium tumefaciens* cultures carrying binary plasmids expressing dimeric HLVd RNAs or mechanically inoculated with in vitro-transcribed dimeric HLVd RNAs. Buffer-inoculated plants served as controls. Hemp seedlings were simultaneously inoculated using the same methods. Reverse transcription (RT)-PCR and northern blot hybridisation analysis of upper uninoculated *A. thaliana* leaves revealed that all inoculated and control plants remained HLVd-negative until 28 days post-inoculation (dpi) (Figure S1 and Table S1). In contrast, HLVd was readily detected in the upper uninoculated leaves of inoculated hemp plants by RT-PCR and northern blot hybridisation (Table S1), with consistent results across two additional repetitions. The failure to infect *A. thaliana* with HLVd (MZ090890) might be attributed to differences in HLVd variants (NC_003611) (Atallah et al. 2024) or plant growth conditions.

Similarly, *A. thaliana* plants were inoculated with HSVd and potato spindle tuber viroid (PSTVd). RT-PCR analysis and northern blot hybridisation of upper uninoculated leaves showed no detectable viroids in *A. thaliana* up to 35 dpi (Figure S1 and Table S1). These findings are consistent with previous reports (Daros and Flores 2004). However, northern blot hybridisation confirmed viroid presence in HSVd-inoculated cucumber plants and PSTVd-inoculated tomato plants (Table S1). These results suggest that systemic viroid infection in *A. thaliana* remains unresolved.

2.2 | Transgenic *A. thaliana* Expressing HSVd

Viroids and noninfectious viroid mutants can establish systemic infections in non-natural hosts through transgenesis (Gomez and Pallas 2006; Wassenegger et al. 1994; Steinbachová et al. 2021; Yamaya et al. 1989). Additionally, dimeric RNA transcripts of viroids like HSVd are efficiently processed into mature circular RNAs and can initiate autonomous replication with low efficiency in transgenic *A. thaliana* (Daros and Flores 2004). To investigate HSVd infectivity in *A. thaliana*, a dimeric head-to-tail HSVd cDNA (X00009) (Figure 1a) was transformed into *A. thaliana*. Of 24 putative transformants selected based on hygromycin resistance and genotyping (Figure S2), seven showed single-copy insertion verified by segregation ratios (~3:1) on hygromycin B-containing plates (Tabe S2). RT-quantitative PCR (RT-qPCR) analysis revealed higher HSVd accumulation levels in line 7 and line 10 (Figure 1b), which were selected for further experiments. No phenotypic differences were observed between transgenic and wild-type plants (Figure 1c).

Northern blot hybridisation following denaturing agarose gel electrophoresis detected HSVd in lines 7 and 10 (Figure 1d). The HSVd accumulation levels in transgenic *A. thaliana* were lower than those in HSVd-infected cucumber plants. However, the signal band sizes were comparable, suggesting that the dimeric HSVd transcripts in transgenic *A. thaliana* were correctly processed, as in cucumber. Attempts to detect circular and linear HSVd RNAs using northern blot hybridisation with denaturing PAGE failed despite repeated trials.

To confirm the presence of mature circular HSVd RNAs, RT-PCR was performed on RNAs treated with RNase R, which specifically degrades linear RNAs (Liu et al. 2023; Ye et al. 2015). Controls included *A. thaliana* circular RNA (chr2:13037381|13038219) and the *ACTIN2* gene (Chen et al. 2017; Zhang et al. 2020). Divergent primers successfully amplified chr2:13037381|13038219 in cDNA but not in genomic DNA, whereas convergent primers amplified both (Figure S3a). Untreated RNAs allowed amplification of both circular and linear forms of chr2:13037381|13038219. Following RNase R treatment, divergent primers amplified only circular RNA, while linear *ACTIN2* was not amplified, confirming linear RNA digestion. Under these conditions, HSVd was amplified using divergent primers (Figure 1e and Figure S3b), verifying the presence of circular HSVd RNAs in transgenic plants.

These results confirmed that dimeric viroid transcripts could be correctly processed into the circular (+) monomers by *A. thaliana* RNase and RNA ligase (Daros and Flores 2004). Cloning and sequencing of RNase R-treated HSVd amplification products showed that most sequences (33/36) were identical to the original cDNA insert, with only three containing minor mutations (Figure S4). These results imply that HSVd replication efficiency in *A. thaliana* is low, consistent with previous observations (Daros and Flores 2004).

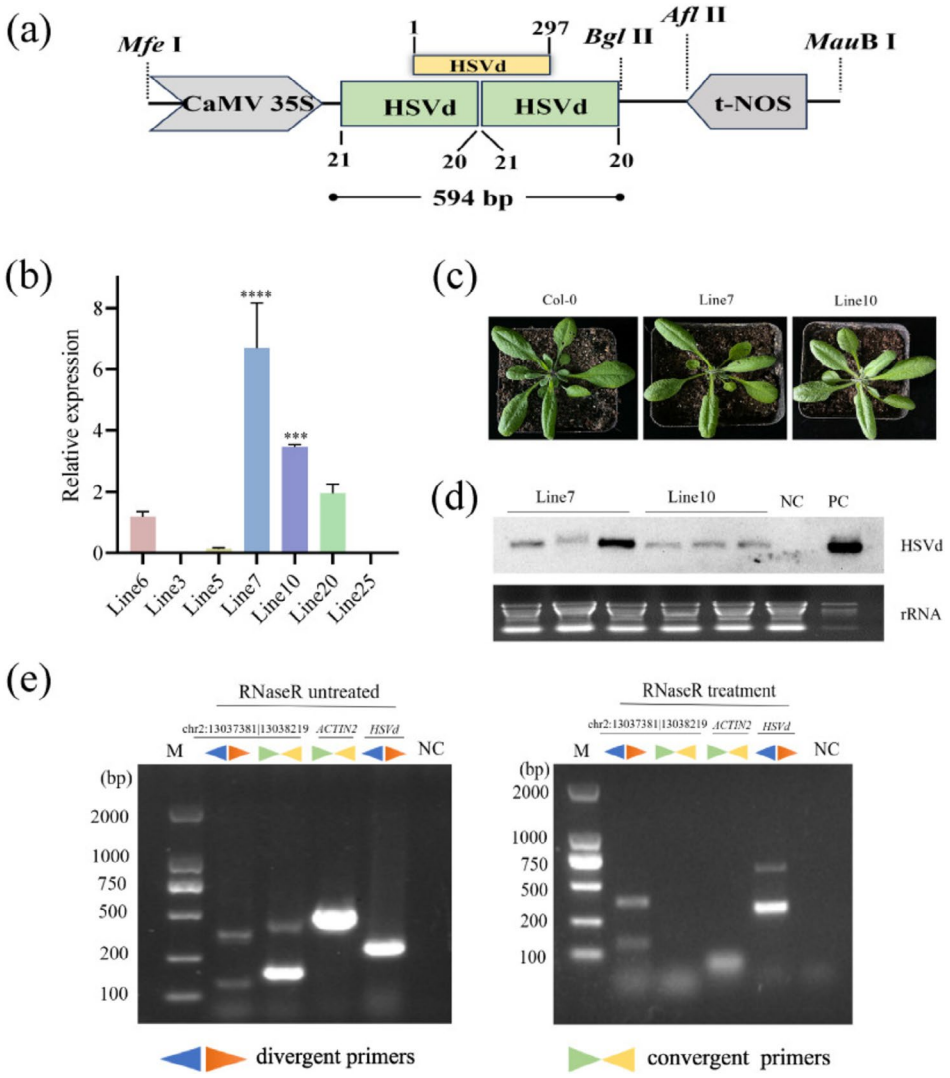

FIGURE 1 | Mature circular hop stunt viroid (HSVd) RNAs are present in transgenic *Arabidopsis thaliana* plants. (a) Schematic representation of the pCAM1305-HSVd construct used for *A. thaliana* transformation. (b) HSVd expression levels in different transgenic lines, measured by reverse transcription (RT)-quantitative PCR and normalised to *ACTIN8* and *SAND* expression levels. Data are shown relative to line 6. Error bars represent the standard deviation of three biological replicates. Statistically significant differences compared to the control are indicated by asterisks (***$p < 0.001$, ****$p < 0.0001$, Student's *t* test). (c) Representative images of Col-0 plants and transgenic *A. thaliana* lines 7 and 10. (d) Northern blot analysis of HSVd in transgenic *A. thaliana* plants. HSVd-infected cucumber serves as a positive control (PC), while wild-type Col-0 is the negative control (NC). (e) Detection of circular HSVd RNAs in transgenic line 7 using RT-PCR following RNase R treatment. Back-to-back triangle primers (divergent) and opposing triangle primers (convergent) were used for validation. Circular RNA of chr2:13037381|13,038,219 and *ACTIN2* serve as controls.

2.3 | Viroid Expression Alters the Expression of Thousands of *A. thaliana* Genes

To investigate the impact of HSVd expression on *A. thaliana* gene expression, transcriptome analysis was conducted on transgenic *A. thaliana* lines 7 and 10, along with wild-type Col-0 plants, using three biological replicates per group. RNA sequencing generated over 38 million reads per library, with Q20 and Q30 scores of 98.9% and 96.8%, respectively, confirming high-quality sequencing data (Table S3). Principal component analysis (PCA) based on gene expression patterns clearly separated the three groups (Figure S5a), demonstrating the biological replicates' consistency and the HSVd transgene's specific effects. Differentially expressed genes (DEGs) were identified using the criteria $\log_2(\text{fold change}) \geq |1|$ and adjusted *p*-value (p_{adj}) ≤ 0.05 (Figure 2 and Table S3). The results were partially validated through RT-qPCR analysis of eight key RNA silencing pathway genes (Figure S5b,c and Table S3) using *EF1α* as a reference.

Transgenic lines 7 and 10 exhibited 6517 and 6378 DEGs, respectively, compared to Col-0 (Figure 2a,b). DEGs accounted for over 25% of detected genes, a higher proportion than the 16% reported in HSVd-infected cucumber (Xia et al. 2017). In addition, transgenic lines 7 and 10 shared more than a half of both the up- and downregulated DEGs (Figure 2c), indicating the consistency of the effect of the HSVd transgene on *A. thaliana* gene expression. These findings indicate that HSVd expression substantially influences the global transcriptome of *A. thaliana*.

Gene Ontology (GO) analysis (corrected $p < 0.05$) revealed enriched biological processes (BP), cellular components (CC), and molecular functions (MF) among DEGs (Table S4). Upregulated DEGs were associated with cellular responses to oxygen levels, metabolic processes, plasma membranes, cell walls, and binding/catalytic activities. Downregulated DEGs were primarily linked to photosynthesis, thylakoid components, and chloroplast structures. These enriched terms largely overlap with those observed in HSVd-infected cucumber (Marquez-Molins et al. 2023; Xia et al. 2017), highlighting similarities in viroid-induced host responses. KEGG pathway analysis (corrected $p < 0.05$) (Table S5) identified enriched pathways in plant metabolism, hormone signalling, pathogen interactions and MAPK signalling (Figure 3a,b), further aligning with results from

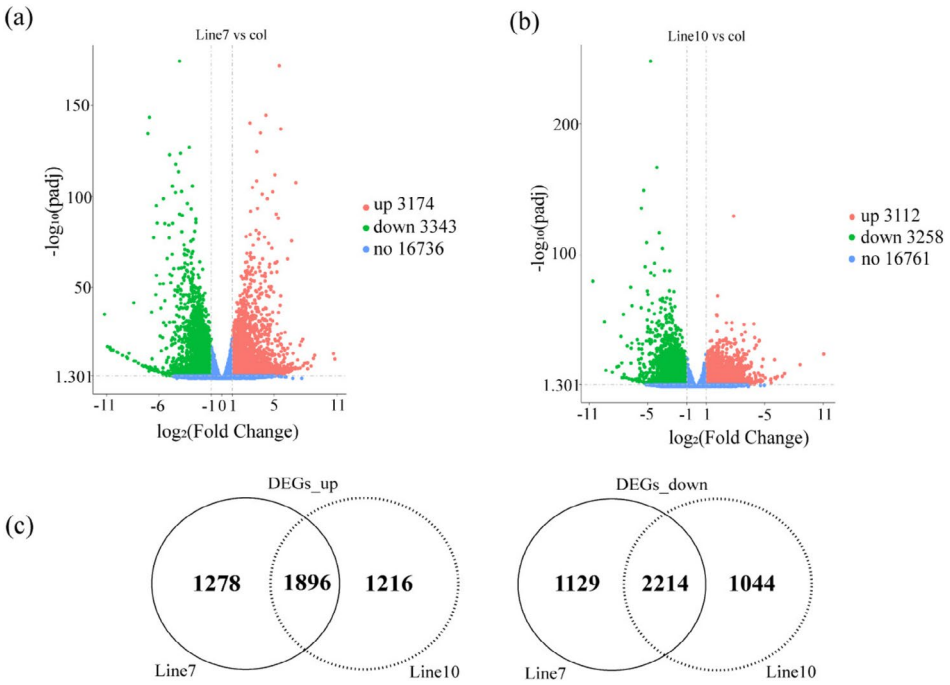

FIGURE 2 | Differential gene expression analysis. (a) Volcano plot depicting differentially expressed genes (DEGs) between HSVd-expressing line 7 and Col-0. The *x*-axis represents the $\log_2$(fold change), and the *y*-axis shows the negative logarithm of the adjusted *p*-value ($-\log_{10}[p_{adj}]$). Points above the threshold lines indicate DEGs with significant changes, with upregulated genes shown in red and downregulated genes in green. Genes with non-significant changes are shown in grey. (b) Volcano plot depicting DEGs between HSVd-expressing line 10 and Col-0. (c) Venn diagram illustrating the overlap of upregulated DEGs (DEGs-up) and downregulated DEGs (DEGs-down) in line 7 and line 10. Each circle represents the set of DEGs identified in a specific experimental condition compared to the control (Col), with overlapping areas showing the co-expressed DEGs common to both conditions.

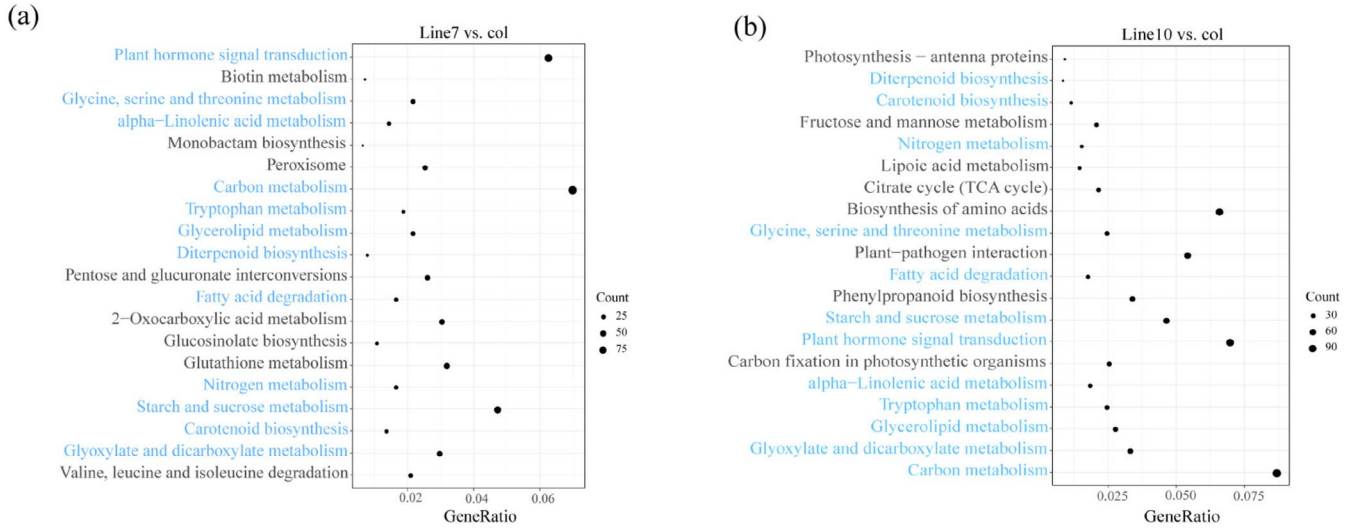

FIGURE 3 | Enriched KEGG pathways (corrected *p*-value < 0.05) of differentially expressed genes in HSVd-expressing *Arabidopsis thaliana* compared to wild-type Col-0 plants. (a) Enriched pathways for line 7, with shared pathways between line 7 and line 10 highlighted in blue. (b) Enriched pathways for line 10.

HSVd-infected cucumber systems (Marquez-Molins et al. 2023, Xia et al. 2017).

2.4 | Loss-Of-Function of DCLs Reduces HSVd Expression Levels in Transgenic *A. thaliana*

Transgenic *A. thaliana* expressing HSVd serves as a valuable model for exploring viroid–host interactions by crossing with mutant lines. Transgenic lines 7 and 10 were crossed with *A. thaliana* mutants deficient in *DCL* genes (*dcl2/3*, *dcl2/4* and *dcl2/3/4*). Self-fertilisation of F_1 populations and genotyping of F_2 generations produced single, double and triple *DCL* mutant lines expressing HSVd. These mutants exhibited phenotypes consistent with their respective parental *DCL* mutants (Figure S6a). Northern blot hybridisation detected HSVd only in transgenic *A. thaliana* but not in *DCL* mutant lines, suggesting that HSVd accumulation in these mutants is extremely low or undetectable. RT-qPCR confirmed these observations (Figure S6b). This contrasts with previous findings that loss-of-function or downregulation of *DCL* genes enhances viroid accumulation (Katsarou et al. 2016; Suzuki et al. 2019; Zhang et al. 2024).

2.5 | Transgenic *A. thaliana* Produces Minimal Viroid-Derived Small RNAs

The low replication efficiency of viroids in transgenic *A. thaliana* (Daros and Flores 2004) may explain the reduced HSVd accumulation in *DCL* mutants. Low replication efficiency probably results in fewer double-stranded RNA intermediates, limiting the production of viroid-derived small RNAs (sRNAs) and attenuating RNA silencing activation.

To quantify HSVd-derived sRNAs, sRNA sequencing was performed on transgenic lines 7 and 10 and wild-type plants. The sequencing generated over 10 million reads per library, with Q20 and Q30 scores of 99.4% and 97.8% (Table S6), respectively, confirming high-quality sequencing data. Only several HSVd-derived sRNAs were obtained in wild-type plants, which should be occasionally generated from the *A. thaliana* genome. In contrast, the 21–24 nucleotide (nt) sRNAs that perfectly matched the HSVd genome (X00009) were detected in transgenic lines with 169–1178 total reads (Table S6). These sRNAs were dominated by 21 nt and 22 nt, followed by 24 nt. The similar size distribution of HSVd-derived sRNA with previous observations (Gomez and Pallas 2010; Navarro et al. 2009; Zhang et al. 2020) supports the reliability of sRNA-sequencing and the biosynthesis of HSVd-derived sRNA in transgenic *A. thaliana*. Although HSVd-derived sRNAs were synthesised in transgenic *A. thaliana*, the amount (16–99 reads per million) was markedly lower than that in HSVd-infected cucumber, hop and grapevine (Gomez and Pallas 2010; Marquez-Molins et al. 2023; Navarro et al. 2009; Zhang et al. 2020).

The amount of sRNA from the plus and the minus strand was similar (Figure 4a and Table S6), indicating that HSVd minus-strand was synthesised in transgenic *A. thaliana* and double-stranded replication intermediates should also be synthesised and processed into sRNA. These results support the viroid replication in transgenic *A. thaliana* (Daros and Flores 2004). Distribution patterns of both plus and minus sRNA along the HSVd genome were similar in the two transgenic lines (Figure 4b). However, they are not completely consistent with previous observations (Gomez and Pallas 2010, Marquez-Molins et al. 2023, Navarro et al. 2009, Zhang et al. 2020), especially hotspots, for example, at the position of 230. The differences in plant and viroid variant may cause this discrepancy. Together, these results indicate inefficient synthesis of double-stranded replication intermediates, suggesting extremely low viroid replication efficiency. The possibility of rapid degradation of HSVd-derived sRNAs, though unlikely, cannot be completely excluded.

3 | Discussion

The model plant *A. thaliana* is an appealing system for viroid research. Although most attempts to inoculate viroids into *A. thaliana* have failed (Daros and Flores 2004; Ma 2022), systemic infection by HLVd has been reported in *A. thaliana* (Atallah et al. 2024), keeping the question open. In this study, both mechanical and agroinfiltration methods were used to inoculate HLVd, HSVd and PSTVd into *A. thaliana* (Col-0 type). Despite repeating the experiments three times for each viroid, systemic infection was not achieved. Similarly, PSTVd failed to establish systemic infection even in eight *A. thaliana* mutants (*dcl2-1*, *dcl4-2 t*, *dcl2-1/dcl3-1*, *dcl3-1/dcl4-2 t*, *rdr2-2*, *rdr6-15*, *ago2-1*, *sgs3-14*) involved in the RNA silencing pathway (Ma 2022). Although environmental conditions (e.g., humidity, temperature and light) varied slightly between trials, the failure of infection suggests that if systemic viroid infection in *A. thaliana* is possible, the required conditions must be highly stringent. Overall, establishing systemic infection in *A. thaliana* remains a significant challenge, limiting its direct use for viroid studies.

Despite these limitations, the transgenic expression of viroids in *A. thaliana* can, to some extent, mimic systemic infection. Previous studies demonstrated that the dimeric cDNA of several pospiviroids, when genetically transformed into *A. thaliana*, was transcribed and efficiently processed into mature circular genome RNAs (Daros and Flores 2004). Our findings corroborate this observation, showing that HSVd transgene (Figure 1) expression was easily detected in *A. thaliana* via northern blotting using a DIG-labelled complementary riboprobe. This supports the potential of viroid-expressing *A. thaliana* as a model system for viroid research. Indeed, this approach has been successfully used to elucidate molecular mechanisms of viroid replication (Gas et al. 2007; Nohales et al. 2012).

Furthermore, transcriptomic analysis revealed that HSVd expression altered the expression of approximately 25% of *A. thaliana* genes, affecting pathways related to metabolism, hormone signalling, defence responses and RNA silencing (Figure 2 and Table S3). These changes mirror responses observed in HSVd-infected cucumber (Marquez-Molins et al. 2023; Xia et al. 2017) and other viroid-infected plants (Joubert et al. 2022). Pathway enrichment analysis identified similarities in plant metabolism, biosynthesis, hormone signalling, plant–pathogen interactions,

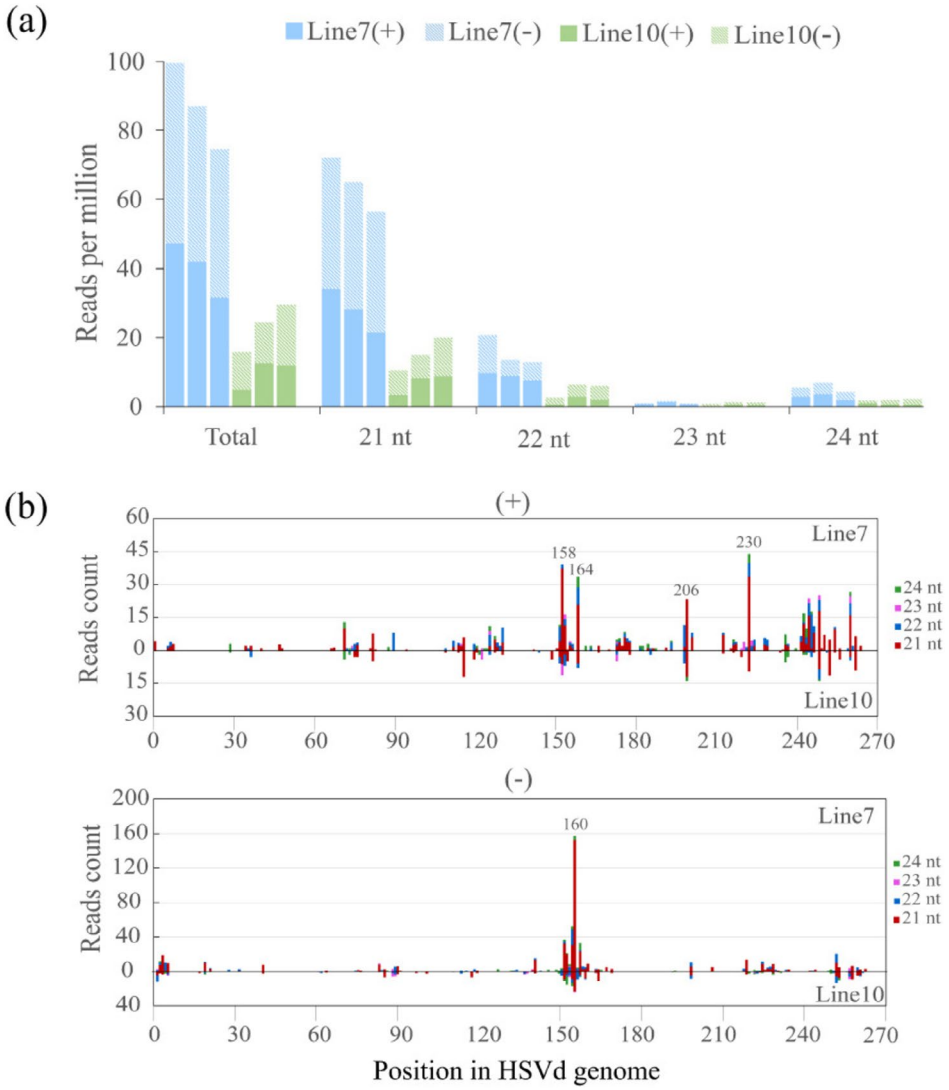

FIGURE 4 | Integration of hop stunt viroid (HSVd) affects the biogenesis of HSVd-sRNAs. (a) The amount (reads per million) of total HSVd-sRNAs and 21–24 nucleotide (nt) HSVd-sRNAs in the transgenic *Arabidopsis thaliana* lines 7 and 10. Each sample has three biological replicates. (b) Distribution profiles of HSVd-sRNAs against the HSVd genome in lines 7 and 10.

and MAPK signalling (Figure 3). This resemblance underscores the value of viroid-expressing *A. thaliana* for studying viroid–host interactions.

This system is particularly advantageous for identifying viroid-binding host factors. Viroids lack protein-coding capacity and depend entirely on host factors for replication, movement and pathogenicity. In systems with systemic viroid infection, many viroid-binding proteins are probably associated with replication. However, in *A. thaliana*, inefficient viroid replication (Daros and Flores 2004) minimises the involvement of replication-associated factors. Although longer-than-unit antisense viroid RNAs were detected (Daros and Flores 2004), HSVd-derived sRNAs were produced in only limited amounts (Figure 4 and Table S6). This suggests that double-stranded RNA intermediates required for efficient replication are either synthesised at extremely low levels or not at all in transgenic *A. thaliana*. Additionally, viroid systemic movement seems to be restricted in *A. thaliana* (Daros and Flores 2004). This partial uncoupling of replication and movement in transgenic *A. thaliana* provides an opportunity to investigate host factors that influence viroid accumulation and processing.

Our observation that HSVd-expressing *A. thaliana* produces a similar number of plus- and minus-strand HSVd-derived sRNAs per plant (Figure 4 and Table S6) offers insights into the biosynthesis of viroid sRNAs. In addition to double-stranded RNAs synthesised during replication by Pol II or during RNA interference (RNAi)-mediated defence by RNA-dependent RNA polymerase (RDR) (Di Serio et al. 2023, 2009; Navarro et al. 2021, 2009), mature viroid genomic RNAs that fold into stem-loop structures similar to microRNA precursors (Itaya et al. 2007) are recognised to be a template for viroid sRNAs. In our study, mature HSVd genomic RNAs were synthesised (Figure 1e), but the amount of plus-strand HSVd-derived sRNAs was similar to, rather than higher than, that of minus-strand sRNAs. These findings suggest that mature HSVd genomic RNAs are suboptimal substrates for *A. thaliana* DCLs, whereas double-stranded replication intermediates are the primary source of viroid-derived sRNAs (Gomez and Pallas 2007; Gomez et al. 2009).

4 | Experimental Procedures

4.1 | Viroid and Plant Materials

Plants (*A. thaliana*, tomato cv. Rutgers, cucumber cv. Suyo, and hemp) were grown in a controlled environment with a 16-h light/8-h dark photoperiod at 22°C under 80% relative humidity. Fully expanded cotyledons of tomato, cucumber and hemp seedlings, 1 or 2 weeks old, and the 8th to 10th rosette leaves of *A. thaliana* were inoculated by viroid. Mechanical inoculation used the inoculum generated via in vitro transcription (Xia et al. 2017) of dimeric cDNAs of HSVd (X00009), PSTVd (MK303581) and HLVd (MZ090890) cloned into the pGEM-T vector (TaKaRa). Additionally, dimeric cDNAs of HSVd were cloned into the binary plasmid pCAM1305.1, while PSTVd and HLVd were cloned into the binary plasmid pCAM1300 for agroinfiltration (Zhang et al. 2024).

4.2 | Transgenesis of HSVd in *A. thaliana* and Crosses With DCL-Deficient Mutants

Dimeric cDNAs of HSVd cloned into the binary plasmid pCAM1305.1 for transgenesis in *A. thaliana* (Col-0). The recombinant plasmid pCAM1305-HSVd (Figure 1a) was transformed into *A. tumefaciens* GV3101 and introduced into *A. thaliana* using the floral dip method (Clough and Bent 1998). T_3 generation transgene seeds were screened by PCR (Table S7). Two HSVd-expressing *A. thaliana* parental lines, line 7 and line 10, were selected based on high HSVd accumulation levels and used for crosses with *A. thaliana* mutants deficient in DCL genes (*dcl2/3*, *dcl2/4*, *dcl3/4*, and *dcl2/3/4*) generated by T-DNA insertion (SALK_064627 for *dcl2-1*; WiscDsLox245A05 for *dcl3-2*; GABI_160G05 for *dcl4-2*) in the Col-0 background. Crosses were performed by emasculating flowers of the female parent to remove anthers, followed by careful transfer of pollen from the male parent to the stigma. F_2 seeds were screened for hygromycin resistance and genotyped.

4.3 | RNA Extraction, RT-PCR, Cloning, and Sequencing

Total RNA was extracted from upper non-inoculated leaves (14, 28 and 35 dpi) using TRIzol reagent (TransGen Biotech) according to the manufacturer's protocol. RNA quality was evaluated by agarose gel electrophoresis and quantified using the Nano300 spectrophotometer (Allsheng). First-strand cDNA synthesis was performed with M-MLV reverse transcriptase (Promega) and random hexamer primers. PCR amplification of the HSVd genome was conducted using Taq or Pfu DNA polymerase (Vazyme Biotech) (Table S7). PCR products were cloned into the pTOPO vector for sequencing.

4.4 | RT-qPCR

Total RNA (1 μg) was treated with DNase I to remove genomic DNA and used as a template for cDNA synthesis using the HiScript II 1st Strand cDNA Synthesis Kit (Vazyme) with random hexamers following the manufacturer's instructions. Real-time qPCR was performed with SYBR Green PCR Master Mix (TransGen). Housekeeping genes, including *ACTIN8* (*AT1G49240*), *SAND* (*AT3G28390*) and *EF1α* (*AT5G60390*) (Gao et al. 2018; Han et al. 2013; Liu et al. 2022), were used for normalisation. RNA silencing-related genes included *AGO1* (*AT1G48410*), *AGO2* (*AT1G31280*), *RDR1* (*AT1G14790*), *RDR6* (*AT3G49500*), *DCL1* (*AT1G01040*), *DCL2* (*AT3G03300*), *DCL3* (*AT3G43920*) and *DCL4* (*AT5G20320*) (Incarbone et al. 2023; Liu et al. 2022). Relative expression levels were calculated using the $2^{-\Delta\Delta Ct}$ method (Livak and Schmittgen 2001). All experiments were conducted in triplicate. RT-qPCR primers are provided in Table S7.

4.5 | Northern Blot Hybridisation and Circular RNA Determination

Northern blot analysis was conducted using a digoxigenin-labelled complementary riboprobe, as previously described (Zhang et al. 2023). Circular HSVd RNAs were detected via denaturing polyacrylamide gel electrophoresis (PAGE) followed by northern blot hybridisation (Daros and Flores 2004). Circular RNA detection was further validated by RT-PCR using divergent primers (Table S7) combined with RNase R treatment (Beyotime), which degrades linear RNAs (Liu et al. 2023; Ye et al. 2015). Total RNA (1 μg) was treated with RNase R (3 U) at 37°C for 40 min, followed by inactivation at 72°C for 10 min. *ACTIN2* (*AT3G18780*) and a reference sequence within gene *AT5G01920* (chr2: 1303738|13038219) were used as controls (Zhang et al. 2020).

4.6 | RNA And Small RNA Sequencing

Leaves from wild-type and HSVd-expressing *A. thaliana* plants were collected at the full-flowering stage (approximately 45 days after planting) for RNA extraction. Three biological replicates were prepared for each group. For RNA sequencing, paired-end libraries were constructed and sequenced on the Illumina HiSeq 2000 platform (Novogene). Raw reads were processed using fastp to remove adapter sequences, reads containing poly-N, and low-quality reads, resulting in high-quality clean reads. Clean reads were mapped to the *A. thaliana* reference genome (https://ftp.ensemblgenomes.ebi.ac.uk/pub/plants/release-56), using HISAT2 v. 2.0.5 with default parameters (Goldstein et al. 2016). Gene expression levels were quantified using featureCounts (1.5.0-p3), and differential gene expression analysis was performed using DESeq2 v. 1.20.0 (Anders and Huber 2010), which applies a negative binomial distribution model to determine DEGs. The Benjamini and Hochberg method was used to adjust *p*-value for controlling the false discovery rate, and genes with $\log_2$(-fold change) $\geq |1|$ and adjusted *p*-value (p_{adj}) ≤ 0.05 were considered differentially expressed (Anders and Huber 2010).

For sRNA sequencing, sRNAs (18–50 nt) were purified from total RNA and used to construct a library with a TruSeq Small RNA Library Prep Kit (Illumina). Sequencing was performed on the Illumina HiSeq 2000 platform, generating 50 bp single-end reads. Adapter sequences were trimmed using Cutadapt, and high-quality reads were aligned to the HSVd genome (X00009) by Bowtie without mismatch to analyse their expression and distribution on the reference (Langmead et al. 2009).

Acknowledgements

This study was funded by grants from the National Natural Science Foundation of China (32072395).

Conflicts of Interest

The authors declare no conflicts of interest.

Data Availability Statement

Raw sequencing data from the RNA-seq and small RNAseq experiment have been deposited at the NCBI SRA (http://www.ncbi.nlm.nih.gov/sra/) under accession number PRJNA1205795.

References

Anders, S., and W. Huber. 2010. "Differential Expression Analysis for Sequence Count Data." *Genome Biology* 11: R106.

Atallah, O. O., S. M. Yassin, and J. Verchot. 2024. "New Insights Into Hop Latent Viroid Detection, Infectivity, Host Range, and Transmission." *Viruses* 16: 30.

Chen, G., J. Cui, L. Wang, Y. Zhu, Z. Lu, and B. Jin. 2017. "Genome-Wide Identification of Circular RNAs in *Arabidopsis thaliana*." *Frontiers in Plant Science* 8: 1678.

Clough, S. J., and A. F. Bent. 1998. "Floral Dip: A Simplified Method for *Agrobacterium*-Mediated Transformation of *Arabidopsis thaliana*." *Plant Journal* 16: 735–743.

Daros, J. A., and R. Flores. 2004. "*Arabidopsis thaliana* Has the Enzymatic Machinery for Replicating Representative Viroid Species of the Family *Pospiviroidae*." *Proceedings of the National Academy of Sciences of the United States of America* 101: 6792–6797.

Di Serio, F., A. Gisel, B. Navarro, et al. 2009. "Deep Sequencing of the Small RNAs Derived From Two Symptomatic Variants of a Chloroplastic Viroid: Implications for Their Genesis and for Pathogenesis." *PLoS One* 4: e7539.

Di Serio, F., R. A. Owens, B. Navarro, et al. 2023. "Role of RNA Silencing in Plant–Viroid Interactions and in Viroid Pathogenesis." *Virus Research* 323: 198964.

Gao, H., M. Yang, H. Yang, et al. 2018. "*Arabidopsis* ENOR3 Regulates RNAi-Mediated Antiviral Defense." *Journal of Genetics and Genomics* 45: 33–40.

Gas, M. E., C. Hernandez, R. Flores, and J. A. Daros. 2007. "Processing of Nuclear Viroids In Vivo: An Interplay Between RNA Conformations." *PLoS Pathogens* 3: e182.

Goldstein, L. D., Y. Cao, G. Pau, M. Lawrence, and R. Gentleman. 2016. "Prediction and Quantification of Splice Events From Rna-Seq Data." *PLoS One* 11: e0156132.

Gomez, G., G. Martinez, and V. Pallas. 2009. "Interplay Between Viroid-Induced Pathogenesis and RNA Silencing Pathways." *Trends in Plant Science* 14: 264–269.

Gomez, G., and V. Pallas. 2006. "Hop Stunt Viroid Is Processed and Translocated in Transgenic *Nicotiana benthamiana* Plants." *Molecular Plant Pathology* 7: 511–517.

Gomez, G., and V. Pallas. 2007. "Mature Monomeric Forms of Hop Stunt Viroid Resist RNA Silencing in Transgenic Plants." *Plant Journal* 51: 1041–1049.

Gomez, G., and V. Pallas. 2010. "Noncoding RNA Mediated Traffic of Foreign mRNA Into Chloroplasts Reveals a Novel Signaling Mechanism in Plants." *PLoS One* 5: e12269.

Han, B., Z. Yang, M. K. Samma, R. Wang, and W. Shen. 2013. "Systematic Validation of Candidate Reference Genes for qRT-PCR Normalization Under Iron Deficiency in *Arabidopsis*." *Biometals* 26: 403–413.

Incarbone, M., G. Bradamante, F. Pruckner, et al. 2023. "Salicylic Acid and RNA Interference Mediate Antiviral Immunity of Plant Stem Cells." *Proceedings of the National Academy of Sciences of the United States of America* 120: e2302069120.

Itaya, A., X. H. Zhong, R. Bundschuh, et al. 2007. "A Structured Viroid RNA Serves as a Substrate for Dicer-Like Cleavage to Produce Biologically Active Small RNAs but Is Resistant to RNA-Induced Silencing Complex-Mediated Degradation." *Journal of Virology* 81: 2980–2994.

Joubert, M., N. van den Berg, J. Theron, and V. Swart. 2022. "Transcriptomics Advancement in the Complex Response of Plants to Viroid Infection." *International Journal of Molecular Sciences* 23: 7677.

Katsarou, K., E. Mavrothalassiti, W. Dermauw, T. Van Leeuwen, and K. Kalantidis. 2016. "Combined Activity of DCL2 and DCL3 Is Crucial in the Defense Against Potato Spindle Tuber Viroid." *PLoS Pathogens* 12: e1005936.

Langmead, B., C. Trapnell, M. Pop, and S. L. Salzberg. 2009. "Ultrafast and Memory-Efficient Alignment of Short DNA Sequences to the Human Genome." *Genome Biology* 10: R25.

Liu, R., Y. Ma, T. Guo, and G. Li. 2023. "Identification, Biogenesis, Function, and Mechanism of Action of Circular RNAs in Plants." *Plant Communications* 4: 100430.

Liu, S., M. Chen, R. Li, et al. 2022. "Identification of Positive and Negative Regulators of Antiviral RNA Interference in *Arabidopsis thaliana*." *Nature Communications* 13: 2994.

Livak, K. J., and T. D. Schmittgen. 2001. "Analysis of Relative Gene Expression Data Using Real-Time Quantitative PCR and the $2^{-\Delta\Delta C(T)}$ Method." *Methods* 25: 402–408.

Ma, J. F. 2022. "The Emerging Value of the Viroid Model in Understanding Plant Responses to Foreign RNAs. [Thesis] Mississippi State University."

Marquez-Molins, J., P. Villalba-Bermell, J. Corell-Sierra, V. Pallas, and G. Gomez. 2023. "Integrative Time-Scale and Multi-Omics Analysis of Host Responses to Viroid Infection." *Plant, Cell & Environment* 46: 2909–2927.

Navarro, B., R. Flores, and F. Di Serio. 2021. "Advances in Viroid–Host Interactions." *Annual Review of Virology* 8: 305–325.

Navarro, B., V. Pantaleo, A. Gisel, et al. 2009. "Deep Sequencing of Viroid-Derived Small RNAs From Grapevine Provides New Insights on the Role of RNA Silencing in Plant–Viroid Interaction." *PLoS One* 4: e7686.

Nohales, M. A., R. Flores, and J. A. Daros. 2012. "Viroid RNA Redirects Host DNA Ligase 1 to Act as an RNA Ligase." *Proceedings of the National Academy of Sciences of the United States of America* 109: 13805–13810.

Somerville, C., and M. Koornneef. 2002. "A Fortunate Choice: The History of *Arabidopsis* as a Model Plant." *Nature Reviews Genetics* 3: 883–889.

Steinbachová, L., J. Matousek, G. Steger, H. Matousková, S. Radisek, and D. Honys. 2021. "Transformation of Seed Non-transmissible Hop Viroids in *Nicotiana benthamiana* Causes Distortions in Male Gametophyte Development." *Plants* 10: 2398.

Suzuki, T., S. Ikeda, A. Kasai, et al. 2019. "RNAi-Mediated Down-Regulation of Dicer-Like 2 and 4 Changes the Response of 'Moneymaker' Tomato to Potato Spindle Tuber Viroid Infection From Tolerance to Lethal Systemic Necrosis, Accompanied by Up-Regulation of miR398, 398a-3p and Production of Excessive Amount of Reactive Oxygen Species." *Viruses* 11: 344.

Wassenegger, M., S. Heimes, and H. L. Sanger. 1994. "An Infectious Viroid RNA Replicon Evolved From an In Vitro-Generated Non-infectious Viroid Deletion Mutant via a Complementary Deletion In Vivo." *EMBO Journal* 13: 6172–6177.

Xia, C. J., S. F. Li, W. Y. Hou, et al. 2017. "Global Transcriptomic Changes Induced by Infection of Cucumber (*Cucumis sativus* L.) With Mild and Severe Variants of Hop Stunt Viroid." *Frontiers in Microbiology* 8: 2427.

Yamaya, J., M. Yoshioka, T. Sano, E. Shikata, and Y. Okada. 1989. "Expression of Hop Stunt Viroid From Its cDNA in Transgenic Tobacco Plants: Identification of Tobacco as a Host Plant." *Molecular Plant–Microbe Interactions* 2: 169–174.

Ye, C. Y., L. Chen, C. Liu, Q. H. Zhu, and L. Fan. 2015. "Widespread Noncoding Circular RNAs in Plants." *New Phytologist* 208: 88–95.

Zhang, J., R. Liu, Y. Zhu, et al. 2020. "Identification and Characterization of circRNAs Responsive to Methyl Jasmonate in *Arabidopsis thaliana*." *International Journal of Molecular Sciences* 21: 792.

Zhang, Y. H., Z. X. Li, Y. J. Du, S. F. Li, and Z. X. Zhang. 2023. "A Universal Probe for Simultaneous Detection of Six Pospiviroids and Natural Infection of Potato Spindle Tuber Viroid (PSTVd) in Tomato in China." *Journal of Integrative Agriculture* 22: 790–798.

Zhang, Y. H., X. X. Tian, H. Y. Xu, et al. 2024. "Knockout of *SlDCL2b* Attenuates the Resistance of Tomato to Potato Spindle Tuber Viroid Infection." *Molecular Plant Pathology* 25: e13441.

Supporting Information

Additional supporting information can be found online in the Supporting Information section.